RESEARCH PAPER

Cancer Biology & Therapy 13:14, 1407–1416; December 2012; © 2012 Landes Bioscience

Preliminary pharmacology of galactosylated chitosan/5-fluorouracil nanoparticles and its inhibition of hepatocellular carcinoma in mice

Mingrong Cheng,[1,4,†] Zheng Liu,[2,†] Tao Wan,[3,†,*] Bing He,[4,*] Bingbing Zha,[5] Jiang Han,[1] Houxiang Chen,[3] Fengxiao Yang,[3] Qing Li,[6] Wei Wang,[1] Hongzhi Xu[4] and Tao Ye[4]

[1]Department of General Surgery; Zhoupu Hospital of Shanghai Pudong New Area; Shanghai, China; [2]Department of Basic Medicine; Medical College of Shaoxing University; Shao xing, China; [3]Biomedical Materials and Engineering Center; Wuhan University of Technology; Wuhan, China; [4]Department of General Surgery; Shanghai Fifth People's Hospital; Fudan University; Shanghai, China; [5]Department of Endocrine; Shanghai Fifth People's Hospital; Fudan University; Shanghai, China; [6]Department of General Medicine; Pujiang hospital of Shanghai; Fifth People's Hospital; Shanghai, China

[†]These authors contributed equally to this work.

Keywords: galactosylated chitosan, nanoparticles, 5-fluorouracil, hepatocellular cancer, pharmacokinetics, apoptosis

Biodegradable polymer nanoparticle drug delivery systems are characterized by targeted drug delivery, improved pharmacokinetic and biodistribution, enhanced drug stability and lowered side effects; these drug delivery systems are widely used for delivery of cytotoxic agents. The galactosylated chitosan (GC)/5-fluorouracil (5-FU) nanoparticle is a nanomaterial made by coupling GC, a polymer known to have the advantages described above, and 5-FU. The GC/5-FU nanoparticle is a sustained release system, it was showed that the peak time, half-life time, mean residence time (MRT) and area of under curve (AUC) of GC/5-FU were longer or more than those of the 5-FU group, but the maximum concentration (Cmax) was lower. The distribution of GC/5-FU in vivo revealed the greatest accumulation in the hepatic cancer tissues, and the hepatic cell was the target of the nanoparticles. Toxicology research showed that the toxicity of GC-5-FU was lower than that of 5-FU in mice. In vivo experiments showed that GC/5-FU can significantly inhibit tumor growth in an orthotropic liver cancer mouse model. GC/5-FU treatment can significantly lower the tumor weight and increase the survival time of mice when compared with 5-FU treatment alone. Flow cytometry and the TUNEL assay revealed that compared with 5-FU, GC/5-FU caused higher rates of G_0-G_1 arrest and apoptosis in hepatic cancer cells.

Introduction

5-fluorouracil (5-FU) is, a water-soluble fluorinated pyrimidine analog still widely used anti-neoplastic agents.[1-3] It is an anti-metabolite of the pyrimidine analog type used for treating various types of solid tumors such as the cancer of liver,[4] stomach,[5] colon,[6] pancreas,[7] breast,[8] etc. alone or in combination. 5-FU is rapidly absorbed through the blood capillaries into systemic circulation with plasma half-life of 10–20 min, hence high doses (400–600 mg/m^2 weekly) are required to achieve therapeutic concentration.[9] This results in relatively low levels of drug near the site of action with the subsequent loss of efficacy and increased risk of serious side effects such as bone marrow depression, gastrointestinal tract reaction, leucopenia and thrombocytopenia.[10,11] 5-FU exhibits its activity by interfere with DNA synthesis by blocking the production of pyrimidine nucleotide dTMP from dUMP in de novo DNA synthesis. This also affects the growth of normal cells and causes adverse side effects. It is desirable to be administered once or twice a week, preferably as a long-acting injectable formulation and targeted to the desired site.[12] The therapeutic efficacy of 5-FU can be increased by binding the drug to carriers such as biodegradable nanoparticles.[13,14]

Biodegradable nanoparticles (NPs) are receiving considerable attention for the delivery of therapeutic drugs. The literature emphasizes the advantages of nanoparticles over microparticles[15] and liposomes.[16] The submicron size of nanoparticles offers a number of distinct advantages over microparticles, including relatively higher intracellular uptake compared with microparticles. To target tumor cells more selectively, active targeting based on antibodies or receptor mediated targeting with cancer specific ligands are developed. Galactosylated chitosan (GC) is a galactose ligand, with chitosan (CS) modifications on the molecular structure.[17] Asialoglycoprotein receptor (ASGPR) is a receptor found on the membrane of hepatocytes facing the sinusoids, with specificity for glycoproteins with galactose or acetyl galactosamine at the end. Each hepatocyte contains approximately 2 million binding sites for ASGR.[18] The binding of the galactose ligand with ASGPR induces liver-targeted gene transfer. Our lab previously synthesized a GC nanoparticle as a gene carrier and showed that the GC nanoparticle can successfully transfer genes

*Correspondence to: Tao Wan and Bing He; Email: wantao@whut.edu.cn and 2011cmr@sina.com
Submitted: 04/22/12; Revised: 08/07/12; Accepted: 08/29/12
http://dx.doi.org/10.4161/cbt.22001

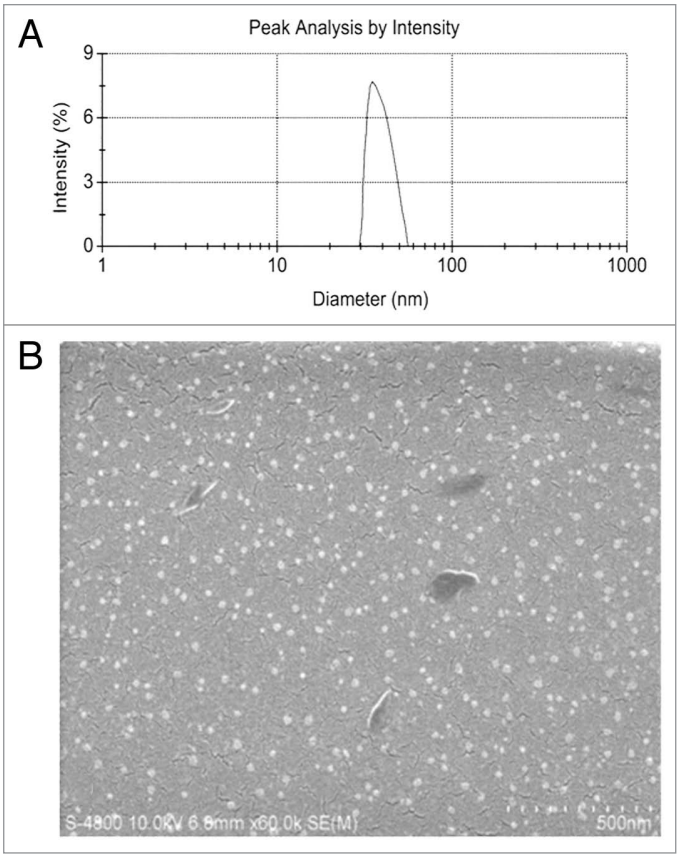

Figure 1. Particle size and scanning electron microscope (SEM) image of GC/5-FU. (**A**) Particle size graph showing the diameter of GC/5-FU (35.19 ± 9.50 nm). (**B**) SEM image of GC/5-FU. The particles show spherical structure with a smooth surface and no adhesion between nanoparticles.

Table 1. Pharmacokinetic parameters of 5-FU and GC/5-FU

Parameters	5-FU	GC/5-FU
Ke (min^{-1})	0.046 ± 0.007	0.002 ± 0.0003
$T_{1/2}$ (min)	16.4 ± 2.51	406.4 ± 54.74
T_{max} (min)	4.47 ± 0.06	125.4 ± 13.71
C_{max} ($\mu g \cdot mL^{-1}$)	57.65 ± 5.22	4.64 ± 0.46
$AUC_{(0\rightarrow\infty)}$ ($\mu g \cdot min \cdot mL^{-1}$)	1074.2 ± 101.12	2701.8 ± 180.69
$MRT_{(0\rightarrow\infty)}$ (min)	16.3 ± 3.08	569.4 ± 39.80

5-Fu, 5-flurouracil; $T_{1/2}$, half-life times; AUC, areas under curve; MRT,: mean residence time; C_{max}, the maximum concentration; T_{max}, the peak time of concentration.

into the liver in vitro and in vivo. In the present study, we also confirmed that this nanoparticle material has a high selectivity for the liver, more stability and sustain release and a low cytotoxicity,[19] and we synthesized GC/5-FU nanoparticles by combining the GC material with 5-FU, GC/5-FU nanoparticles is a sustained release, its peak time, half-life time, mean residence time (MRT) and area of under curve (AUC) were longer or more than those of 5-FU. Meanwhile, distribution of the GC/5-FU in the tissue and toxicity experiment suggested that GC/5-FU was a high targeting drug on the liver cancer with lower toxicity. GC/5-FU nanoparticles can also significantly inhibit the tumor growth in the orthotropic liver cancer mouse model, and this in vivo effect was stronger than that of 5-FU alone. The mechanism underlying GC/5-FU nanoparticles was concluded to be elevated G_0-G_1 arrest and apoptosis.

Results

Synthesis and characterization of GC/5-FU nanoparticles. 5-FU/GC nanoparticles was successfully synthesized, the radius of the nanoparticles was 35.19 ± 9.50 nm, which had a normal distribution (**Fig. 1A**). Electron microscopy showed that the particles were regular spherical shapes, with a smooth surface, a uniform size, and no adhesion between nanoparticles (**Fig. 1B**). The drug loading was 6.12 ± 1.36%, the encapsulation efficiency was 81.82 ± 5.32%, and the Zeta potential was +10.34 ± 1.43 mV. **Figure 2** showed the in vitro release curve of nanoparticles in simulated body fluid (37°C, pH 7.4). A rapid release was observed from time 0 to 12 h, with a cumulative release percentage of 32.4%, presumably due to the diffusion of surface 5-FU into the solution; a smooth slow-release occurred between day 1 and day 8, with a cumulative release percentage of 93.50%, indicating the GC/5-FU nanoparticles have a sustained release effect during days 1 to 8. During days 8 to 10, the release reached a plateau, with a cumulative release percentage of 95.70% at day 10.

Preliminary pharmacokinetics of GC/5-FU in mice. The Cmax of 5-FU group appeared within 5 min, and then the concentration stepped down quickly. The concentration was near 0 after 4–6 h. The concentration of GC/5-FU was slowly increased and reached to the Cmax of it about 2 h, then the concentration stepped down slowly and maintained within 30–60 h. GC/5-FU group's Cmax of 5-FU in plasma were lower than that of the 5-FU group, but the half-life time was obviously longer than that of 5-FU group (**Fig. 3**). **Table 1** showed that besides prolong of half-life, the Tmax, mean residence time (MRT) in the GC/5-FU group were longer than those in the 5-FU group. Meanwhile, the area of under curve reflecting the drug absorption or release into the blood in GC/5-FU group increased significantly and reached 2.7-fold than that of 5-FU group. Taken from above data, we confirmed that GC/5-FU is a sustained release and effective drug which have longer half-time, MRT and AUC.

Determination of in vivo liver-targeting of GC/5-FU. An equation of y = 2.5721x + 0.6851 (r = 0.9956) was derived based on the linear relationship between 5-FU data points ranging from 0.1 to 20 mg/L and the 5-FU peak. The in vivo concentration of 5-FU in mice can be calculated by the above equation.

When the orthotropic liver cancer mouse model had been developed, 5-FU and GC/5-FU were injected through tail vein in model mice or normal mice. Thirty minutes after injection, the 5-FU concentration was measured in the following organs and tissues: heart, liver, spleen, lung, kidney, muscle, brain and liver cancer (only in the mouse model). **Figure 4A** shows that in normal mice the 5-FU concentration in the same tissue showed a significant difference between 5-FU and GC/5-FU

group ($p < 0.01$). The 5-FU concentration in the liver in GC/5-FU group was significantly higher (over 1.5-fold) than that in 5-FU group ($p < 0.01$), while, the 5-FU concentration of GC/5-FU group in other tissues was significantly lower than that of 5-FU group ($p < 0.01$): heart, spleen, lung, kidney, muscle and brain, respectively. In model mice, as shown in **Figure 4B**, the 5-FU concentration of liver and liver cancer tissue in GC/5-FU group was increased significantly than that in 5-FU group ($p < 0.01$), the 5-FU concentration of liver cancer tissue in GC/5-FU group was over 2-fold in 5-FU group. The 5-FU concentration of other tissue in model mice was the same trend as normal mice.

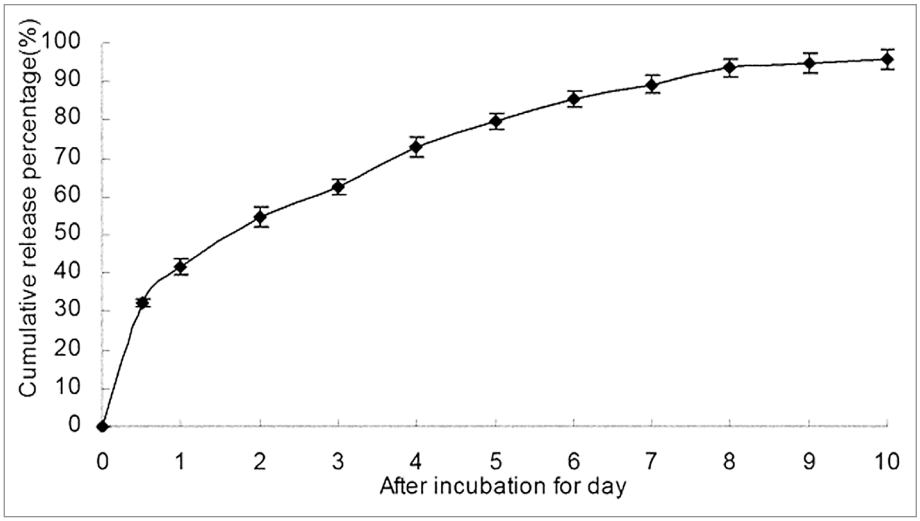

Figure 2. The in vitro release curve of nanoparticles in simulated body fluid (37°C, pH 7.4, n = 3). A rapid release was observed from time 0 to 12 h, with a cumulative release percentage of 32.4%; a smooth slow-release occurred between days 1 and 8, with a cumulative release percentage of 93.50%. During days 8 to 10, the release reached a plateau, with a cumulative release percentage of 95.70% at day 10.

Toxicity of GC/5-FU in mice. In control group, mice displayed different degree toxicity on the mental disorder, drinking, depression and locomotion, even death. Median lethal dose (LD50) means the dose of 50% death on animal, reflecting the degree of drug toxicity. Our results showed that LD50 of 5-FU injection was 197.36 mg/kg and its 95% confident interval was 153.89–240.83 mg/kg. In experiment group, no dead mice were found after administration of GC/5-FU at dose of 775, 912, 1073, 1262 and 1485 mg/kg, respectively. If concentration of GC/5-FU was further increased, more precipitated solid substance would be appear and difficult to take effect on the mice. Meanwhile, 25 μL/g was the maximum volume of injection in mice. Therefore, according to requirement of acute experimental toxicity guidelines of chemical medicine by Chinese Food and Drug Administration, the maximum dose method was to judge the acute toxicity of drug. We continuously observed 20 mice, male and female in half, for 14 d after injection of GC/5-FU at dose of 1,485 mg/kg and no found

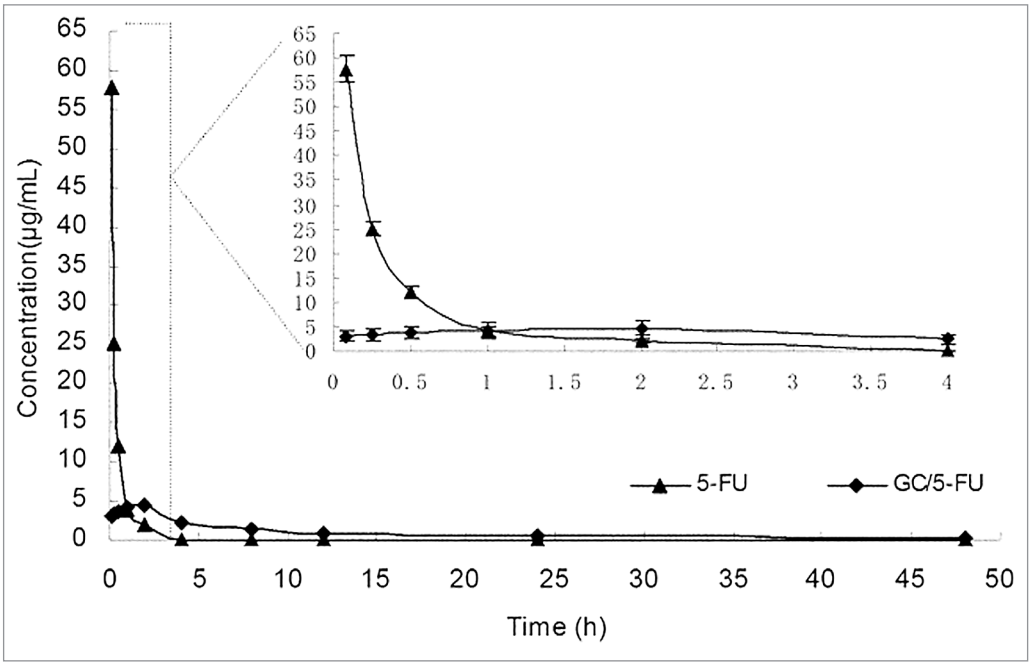

Figure 3. Concentration-time curves of 5-FU and GC/5-FU from 5 min to 48 h in mice after tail vein injection (n = 150). The Cmax of 5-FU group appeared within 5 min, and then the concentration stepped down quickly. The concentration was near 0 after 4–6 h. The concentration of GC/5-FU was slowly increased and reached to the Cmax of it about 2 h, then the concentration stepped down slowly and maintained within 30–60 h. GC/5-FU group's Cmax of 5-FU in plasma were lower than the 5-FU group, but the half-life time was obviously longer than that of 5-FU group.

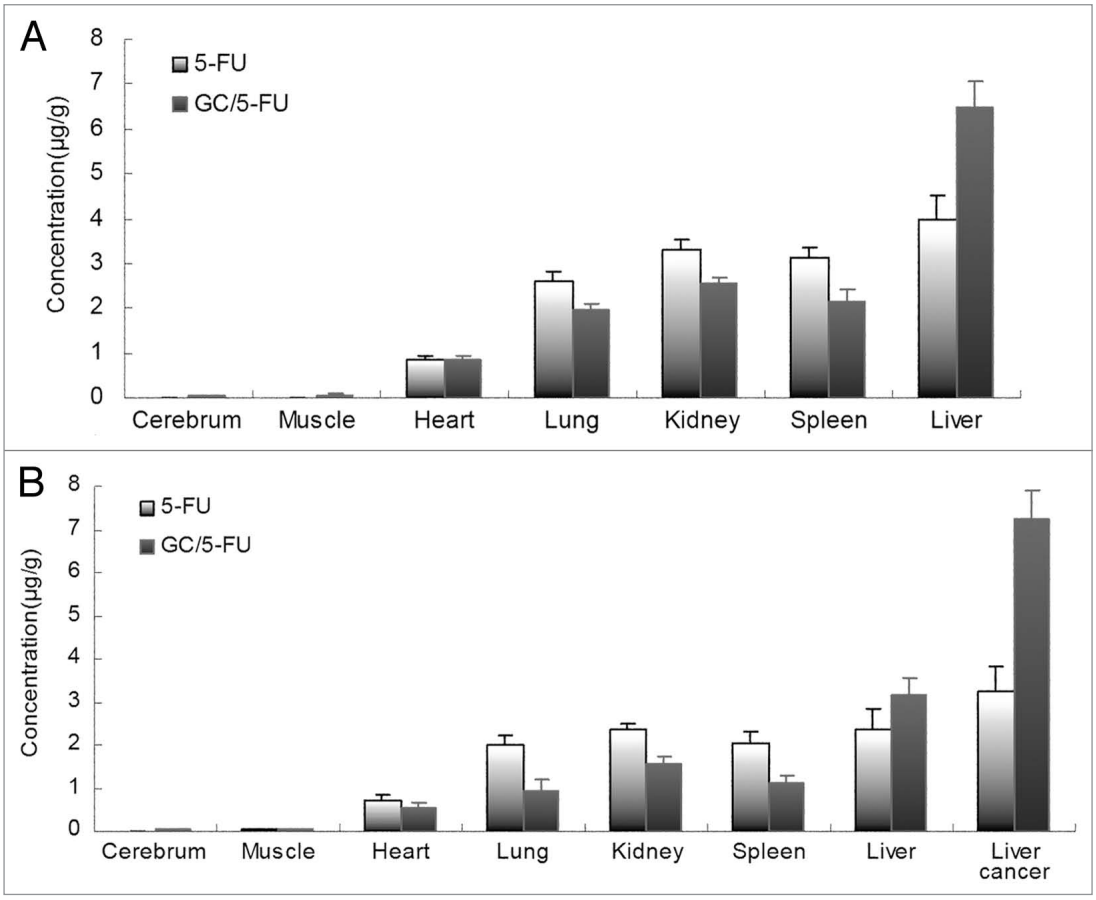

Figure 4. Model mice and normal mice were treated with i.v. 5-FU or GC/5-FU, 5-FU concentration in different tissues was determined 30 min post-injection; results were shown as an average ± standard deviation (n = 5). (**A**) 5-FU concentration in different tissues in normal mice. The 5-FU concentration in the liver in GC/5-FU group was significantly higher (over 1.5-fold) than that in 5-FU group. (**B**) 5-FU concentration in different tissues in model normal mice. The 5-FU concentration of liver and liver cancer tissue in GC/5-FU group was increased significantly than that in 5-FU group, the 5-FU concentration of liver cancer tissue in GC/5-FU group was over 2-fold in 5-FU group.

death of mice. Observation of the final death animal, degeneration and necrosis of viscera were not found in both groups. The maximum dose of GC/5-FU was 1,485 mg/kg, which cannot cause death of mice. Thus, we considered the dose of 1,485 mg/mL as the maximum tolerance dose (MTD) of GC/5-FU. All those results suggested that the toxicity of GC/5-FU is low and it may have potential clinical application.

The effect of GC/5-FU on the tumor mass and survival in the mouse model. The tumor samples were harvested and weighted 15 d post-treatment (**Fig. 5A**). The weight of the tumor in each group was: 0.4361 ± 0.1153 g in GC/5-FU group, 0.7932 ± 0.1283 g in 5-FU group, 1.3989 ± 0.2125 g in GC group and 1.5801 ± 0.2821 g in control group. The difference between the groups was statistically significant ($p < 0.01$). The tumor weight in the GC/5-FU group and the 5-FU were significantly less than those in the GC group and control group ($p < 0.01$); tumors in the GC/5-FU group were significantly less compared with the 5-FU group ($p < 0.01$); however, the tumors in the GC group and the control group were not different ($p > 0.05$).

After the model was developed, the mice were randomly assigned to four groups with 15 mice each, and treated as described above. The survival of the mice was monitored; the mice in all groups demonstrated 100% mortality. The Kaplan-Meier survival curve (**Fig. 5B**) showed that mice in the control group demonstrated 100% mortality, with all the mice dying between days 6 and 14. The median survival time was 12 d. In the GC group, mice also had 100% mortality, with mice dying between days 5 and 16, and the median survival time being 13 d. There was no statistical difference between the survival of mice in the control or GC groups ($p > 0.05$). Mice treated with 5-FU also had 100% mortality, with mice dying between days 13 and 24, with a median survival of 17 d. All mice in the GC/5-FU group died between days 15 and 37, with a median survival time of 30 d. The median survival time of mice treated with either 5-FU or GC/5-FU was significantly longer than that of mice in the GC or control groups; the longest median survival time was seen in the GC/5-FU group ($p < 0.01$ compared with the control, GC and 6-FU groups).

The effect of GC/5-FU on the cell cycle, proliferation and apoptosis of H22 cells. Flow cytometry was used to analyze the liver cancer samples harvested 15 d after beginning treatment. As shown in **Figure 6A and B**, the percentage of cells in

the G_0-G_1 phases was significantly higher in the GC/5-FU- and 5-FU-treated tumors ($p < 0.01$), while the proliferation index (PI) was lower than that in the GC and control groups ($p < 0.01$), suggesting GC/5-FU and 5-FU had an overt anti-proliferative effect and arrested the tumor cells in the G_0–G_1 phases. The PI in the GC/5-FU and 5-FU groups was significantly increased when compared with that in the control and GC groups ($p < 0.01$). Also, the percentage of apoptotic cells of GC/5-FU group was higher than that in the 5-FU group ($p < 0.01$), suggesting that GC is able to enhance the cellular influx of 5-FU and thereby improving the pro-apoptotic effect of 5-FU (**Fig. 6C**).

Apoptosis was detected using the TUNEL assay on the tumor sections. As presented in **Figure 7**, the tumor samples from the control and GC groups showed little apoptosis; the addition of 5-FU induced sporadic apoptosis, while GC/5-FU induced a high degree of apoptosis which showed a clustered distribution. Quantification of the apoptosis index (AI, **Fig. 8**) under a higher magnitude microscopy identified a statistically significant difference between the GC/5-FU group (AI = 21.34%) and the 5-FU group (AI = 14.74%, $p < 0.05$), both of which were higher than that in the GC and control groups ($p < 0.01$).

Discussion

The utilization of nanotechnology and nano-materials in the pharmaceutical field gave rise to the drug-nanoparticle carrier-release system, which is a drug delivery system using nanoparticles as the drug carriers. A particle ranging from 0.1 to 100 nm is considered to be a nanoparticle.[24] The size of a nanoparticle is very important for drug delivery, as the spaces between the cells in various tissues are different: it is now known that the aperture of vascular endothelial within most normal tissues is 2 nm, the aperture of the postcapillary venule is 6 nm, while that of non-continuous tumor blood vessels ranges from 100 to 780 nm.[25,26] The size of the nanoparticles used in this study was approximately 35.19 nm (**Fig. 1A**), which is smaller than most nanoparticles reported,[27] allowing them to enter the space within tumor cells but restricting them from penetrating the normal tissues. SEM analysis revealed a spherical structure with a smooth surface and no adhesion between nanoparticles (**Fig. 1B**), which is consistent with previous reports.[27,28] The drug loading rate of the nanoparticles was determined to be 6.12 ± 1.36%, the encapsulation efficiency was 81.82 ± 5.32%, and the Zeta potential was +10.34 ± 1.43 mV. All those results suggested that GC/5-FU nanoparticle could be considered as a carrier-release drug to treat tumor. However, whether GC/5-FU is a sustain release and higher targeted drug with less toxicity.

Thus, the following experiment in vivo or vitro were performed to reveal the characteristics of GC/5-FU about its preliminary pharmacokinetics including release, distribution, elimination, and its toxicity. First, an experiment was completed to confirm the sustained release effect of GC/5-FU, in vitro. The release curve of GC/5-FU in simulated body fluid showed that the sustained release of the nanoparticle lasted from days 1 to 8. Such sustained release effect makes the drug evenly distributed in the body, which indicates increasing on the half-life of

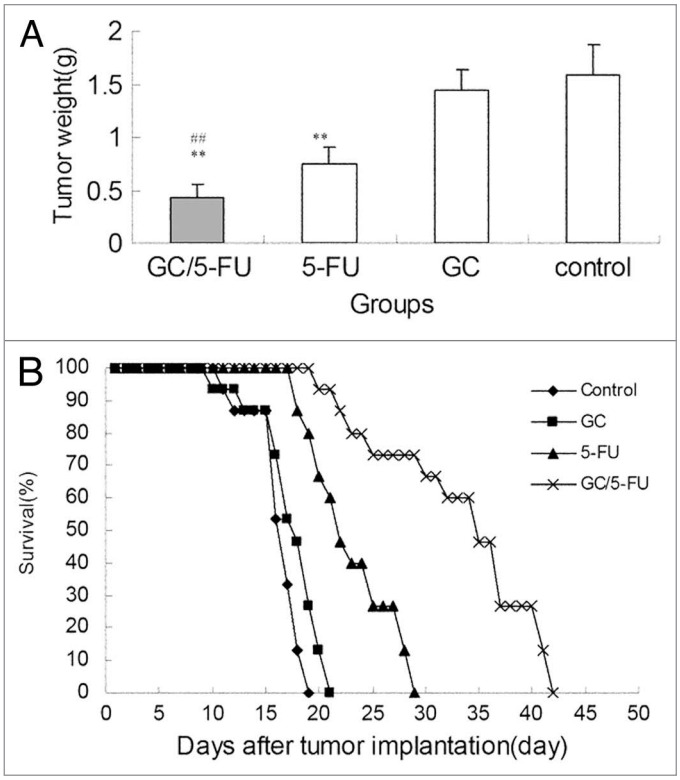

Figure 5. The curative effect of GC/5-FU on liver cancer in the orthotopic transplant model of hepatocellular carcinoma. (**A**) Five days after the tumor was established, GC/5-FU, 5-FU, GC or PBS was given to the mice. Tumor weight was measured at day 10. (**B**)Treatment was given as described previously and the survival was monitored. The median survival for control, GC, 5-FU and GC/5-FU groups were 12, 13, 17 and 30 d, respectively. Compared with control or GC group, **$p < 0.01$; compared with 5-FU group, ##$p < 0.01$.

GC/5-FU in the circulation system and decreasing on the toxic effects of 5-FU on normal tissues.[29] Then, the further change of pharmacokinetic parameters of GC/5-FU in vivo was observed, such as half-life time, the maximum of concentration, mean residence time, etc. In this experiment, pharmacokinetic parameters of 5-FU and its GC nanoparticles in mice showed that GC/5-FU nanoparticles groups' Cmax of 5-Fu in plasma were lower than the 5-FU group, the half-life times and MRT were prolonged and the areas under curve were higher. It indicated that 5-FU, which embeds to GC nanoparticles, slowly released to blood with the carrying nanoparticles slowly degraded. The absorption and disposition in body of nanoparticles is different from macrobead matter because of its small architecture. Maybe it would solve the problem of short plasma half-life, severe side effects with high doses.[30,31] In order to comprehend the pharmacokinetics better, we determined concentration of 5-FU to detect the distribution of GC/5-FU in major organs in our later experiments. These results showed that in normal mice, compared with the 5-FU, the concentration of 5-FU in the liver cancer tissue in GC/5-FU was higher (over 1.5-fold) than in 5-FU group. In model normal mice, the 5-FU concentration of liver and liver cancer tissue in GC/5-FU group was increased

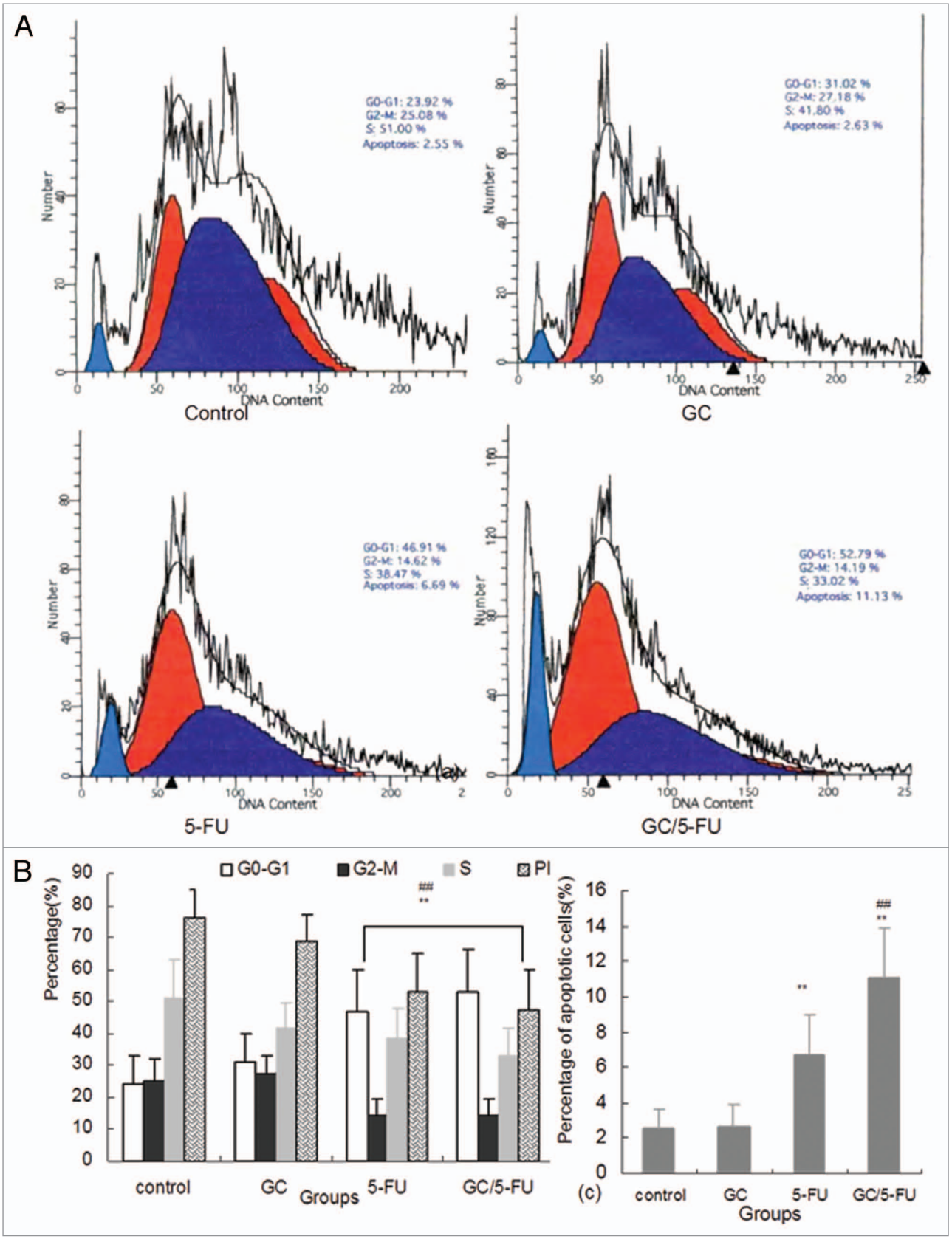

Figure 6. The effects of different treatments on cell cycle, proliferation index and apoptosis index. (**A**) Flow cytometry analysis of cell cycle distribution of H22 cells. (**B**) Quantification of cell cycle distribution and proliferation index of H22 cells. Percentage of cells in G_0–G_1 in the GC/5-FU and 5-FU groups was higher than that in control and GC groups, while the proliferation index decreased significantly ($p < 0.01$). (C) Quantification of apoptosis of H22 in different treatment groups. Compared with control or GC group, **$p < 0.01$; compared with 5-FU group, ##$p < 0.01$.

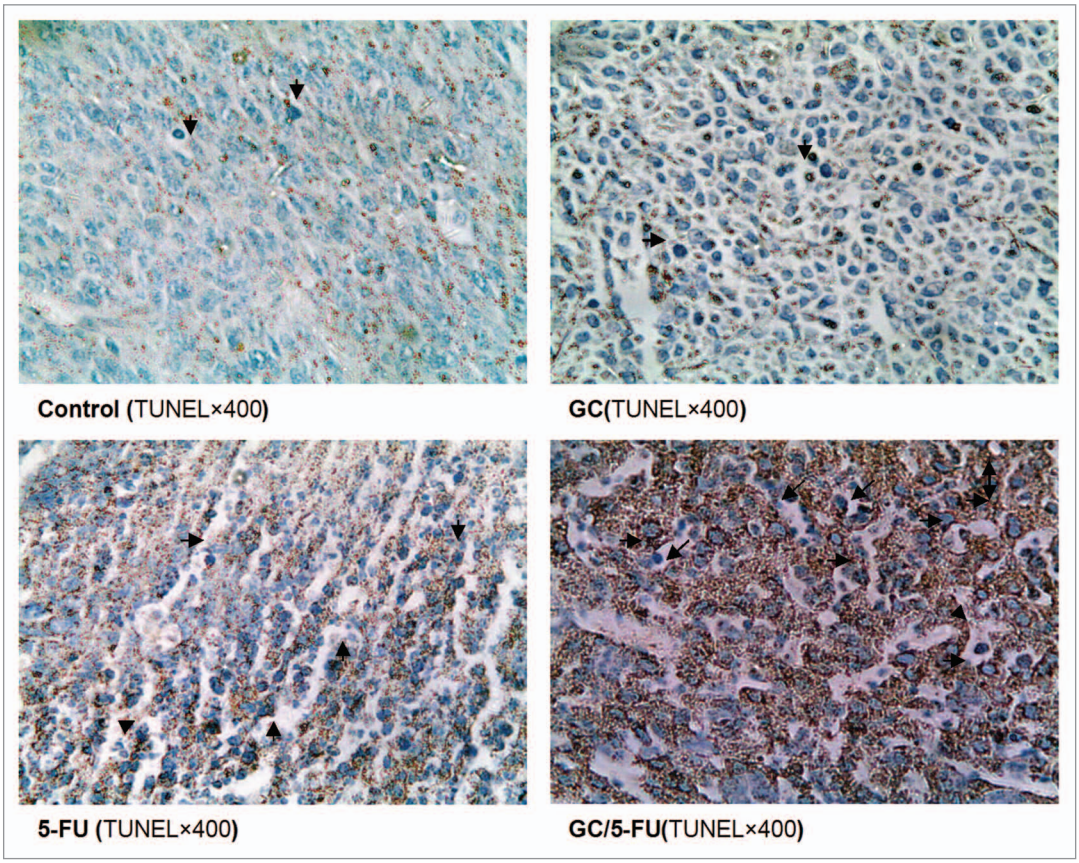

Figure 7. In situ apoptosis detected by TUNEL assay. Few apoptotic cells can be detected in control or GC groups; scattered distributed apoptotic cells can be observed in the 5-FU-treated group and massive clustered apoptotic cells were seen in the GC/5-FU group.

significantly than that in 5-FU group, the 5-FU concentration of liver cancer tissue in GC/5-FU group was over 2-fold in 5-FU group. All those suggested that GC/5-FU has a high targeting on the liver cancer, indicating which would be a potential drug to treat hepatic tumor. Besides investigation on pharmacokinetics of GC/5-FU, we also observe its toxicity or side effects. In present study, it is found that MTD of GC/5-FU is 1,485 mg/kg body weight while LD50 of 5-FU is 197.36 mg/kg, which enough to confirm the toxicity of drug in former was lower than latter. Therefore, GC/5-FU was an effective drug on liver cancer with high targeting and lower toxicity.

In order to evaluate the curative efficiency of intravenously injected GC/5-FU in a liver cancer mouse model, some of the mice were sacrificed and analyzed at day 15 post-injection. As shown in **Figure 5A**, the tumor weight in mice treated with GC/5-FU and 5-FU was significantly obviously less than that in mice treated with GC or control; GC/5-FU-treated tumors were even less than the 5-FU-treated tumors, while the GC- or control-treated tumors did not show any statistically significant difference. The survival of all groups of mice after treatment was monitored, and all mice in all groups died. In the control group, mice died between days 6 and 14, with a median survival 12 d; in the GC group, mice died between days 5 to 16, with a median survival 13 d, showing no difference from the control group (**Fig. 5B**, $p > 0.05$). Mice in the 5-FU group succumbed to tumor-associated death between days 13 and 24, with a median survival time of 17 d, while mice in the GC/5-FU group died between days 15 and 37, with a median survival time of 30 d. The survival time of mice treated with either 5-FU or GC/5-FU was significantly longer than that of mice in the control and GC groups, with the longest survival time seen in the GC/5-FU group ($p < 0.01$). This result suggested that although GC alone cannot affect tumor growth, the conjugation of GC to 5-FU improved the tumor suppressive effect of 5-FU. To determine the mechanism of effect of GC/5-FU nanoparticles on the hepatic cancer, we used flow cytometry and the TUNEL assay to examine tumor cell apoptosis. The results revealed that both 5-FU and GC/5-FU enhanced apoptosis when compared with either control or GC, and compared with 5-FU alone, GC/5-FU further increased the apoptosis index, suggesting that GC improves the pro-apoptotic effect of 5-FU by promoting its entry into the cell. In addition, as shown in **Figure 6A and B**, compared with control and GC treatment, 5-FU and GC/5-FU treatment can increase the percentage of cells in the G_0–G_1 phases ($p < 0.01$) but lower the PI ($p < 0.01$), suggesting 5-FU and GC/5-FU are cytotoxic to proliferating cells by arresting them in the G_0–G_1 phases; this is consistent with previously reported research.[32,33] Therefore, GC facilitates intracellular transport of 5-FU, improving the effects of 5-FU on tumor cell apoptosis and on inhibition of the cell cycle.

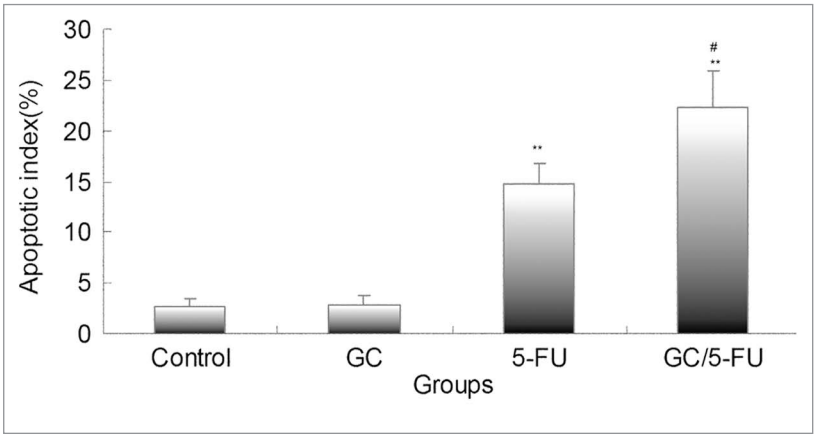

Figure 8. Bar graph showing quantification of the apoptotic index (AI) in hepatic cancer tissues with different treatments. AI increased from control to GC to 5-FU to GC/5-FU ($p < 0.01$). Compared with control or GC group, **$p < 0.01$; compared with 5-FU group, #$p < 0.05$.

Materials and Methods

Reagents. 1-ethyl-3-(3-dimethylaminopropyl) carbodiimide hydrochloride (EDC), Chitosan (CS, degree of deacetylation, > 85%), N-hydroxysuccinimide (NHS), RNase and 5-Bru were purchased from Sigma. GC-5-FU nanoparticle was synthesized and stored by our group. 5-FU was purchased from Shanghai Xudong Haipu Pharmacetutical Co., Ltd. The TUNEL assay kit was from Roche; and the immunohistochemistry kit was from GBI.

Mice and cell lines. The mouse liver cancer cell line (H22) were purchased from the Cancer Institute at Fudan University. BALB/c mice, 7 weeks of age and weighing 20-25 g, were obtained from the Science Department of Experimental Animals of Fudan University in China. All mice were housed in SPF level B animal facility and animal experiments were conducted following the guidelines of the Animal Research Ethics Board of Fudan University.

Synthesis of GC/5-FU. The 5-FU/GC was mixed at a mass ratio of 10:1 in solution, using vortex oscillator (2,500 rpm) for 30 sec; the final concentration of 5-FU was 1.857 mg/mL. The product was kept at room temperature for 30 min to assess for further particle formation. The final product was kept at 4°C. The drug loading and encapsulation efficiency were calculated according to the following equations: drug loading = the amount of 5-FU within nanoparticle/ nanoparticle mass × 100%; encapsulation efficiency = the amount of 5-FU within nanoparticle/ total amount of 5-FU added × 100%.

Preparation of 5-FU standard curve. Standard solution was added to 0.5 mL of serum to make a 5-FU solution with a final concentration of 0.1, 0.2, 0.5, 1.0, 5.0, 10 and 20 mg/L, respectively. Linear regression was used by placing the 5-FU concentration on the x-axis and the measured 5-FU peak area as y-axis.

In vitro release experiment. Nanoparticles (20 mg) were mixed with 30 mL of simulated body fluid (SBF, pH 7.4) in dialysis bags and incubated at 37°C using a shaker with a fixed speed of 60 rpm. Samples were taken at 0.5, 1, 2, 3, 4, 5, 6, 7, 8, 9 and 10 d post-mixing. The optical density (OD) was measured at 265 nm by an automated microplate reader (Bio-Rad). The amount of 5-FU released at different time points was calculated according to a standard absorbance curve. The concentration and cumulative release percentage were calculated according to the standard curve equation. Each experiment was performed in triplicate.

Preliminary pharmacokinetics of GC/5-FU. One hundred and twenty mice were randomly divided into two groups with 60 mice in each group, one group for administration with 5-FU solution (1.857 mg/mL) at a dose of 0.371 mg every mouse and the anther group of GC/5-FU nanoparticles at an equivalent drug dose to the 5-FU group. At 5 and 30 min and 1, 2, 4, 8, 12, 16, 24 and 48 h after administration through tail vein injection, the blood sample was drawn from the neck vein of mice in two groups (six mice in each sub-group), respectively. All blood samples were collected in heparinized tubes and were immediately centrifuged (3,000 r/min, 10 min). Plasma samples were obtained and stored in a 4°C freezer.

Concentration of GC/5-FU in different tissues. To investigate the targeting of GC/5-FU on liver cancer, after the tumor was established in the mouse model, the mice (n = 10) were randomly assigned into 5-FU and GC/5-FU group, with 5 mice in each group. As a control, ten normal mice were also were randomly divided into 5-FU and GC/5-FU group, each group had 5 mice. 5-FU of 15 mg/kg in mice, or GC/5-FU (containing the same 5-FU) was injected through tail veil. Tissues and organs including heart, liver, spleen, lung, kidney, muscle, brain and liver cancer (only in the mouse model) were harvested 30 min post-injection. After washing with saline, 0.5 to 1.0 g of tissues was homogenized and 0.5 mL was taken for determination of 5-FU concentration.

Toxicity of GC/5-FU. A hundred of mice were randomly divided into two groups, each group subdivided into five sub-groups with 10 mice in each sub-group. The acute toxic reaction and the main viscera pathological morphology of mice were evaluated after given 5-FU or GC/5-FU by intravenous injection via vena caudalis with different doses, respectively. In control group, five sub-groups mice were given 5-FU at a dose of 142, 190, 253, 338 and 450 mg/kg, respectively; in the experiment group, GC-5-FU was given at dose of 775, 912, 1,073, 1,262 and 1,485 mg/kg respectively, in each sub-group. We mainly observed the behavior, mental, drinking, sleep, locomotion and number of death from 0 days to 2 weeks. The main viscera pathological morphology of mice was observed by an anatomical structure through the unaided eye. Importantly, we will calculate the LD50 of 5-FU or maximum tolerance dose (MTD) of GC-5-FU at vein injection to evaluate its toxicity for mice.

Animal model. The subcutaneous liver cancer mouse model was established by using the mouse hepatocellular cancer cell line H22. After euthanasia and dissection, fresh fast-growing tumor tissues were minced and made into a tumor cell suspension at the density of 6×10^7/mL. Recipient mice were anesthetized by 20% urethane, followed by an injection of 50 μL of tumor cell

suspension into the liver left lobe capsule. Approximately 2 min after completion of the procedure, when there was no leaking, the abdomen was sutured and the orthotropic liver cancer mouse model was established successfully.[20]

Observation of the curative effect of GC/5-FU in the orthotropic liver cancer mouse model. Five days after the establishment of the hepatic tumor, it reached about 4 to 6 mm in diameter (**Fig. 9**). The mice with tumors were randomly assigned into four groups labeled as control, GC, 5-FU and GC/5-FU. Mice in the control group received 200 μL saline through an intravenous injection. Mice in the GC group received 200 μL GC nanomaterial. Mice in the 5-FU and GC/5-FU groups received 200 μL (containing 0.371 mg 5-FU) 5-FU and GC/5-FU, respectively. The drugs were given continuously for 5 d starting from day 5 after the tumor was established. At day 15, all model mice were sacrificed and the tumor growth was monitored. The remaining 15 mice in each group were kept for survival analysis.

Cell cycle and apoptosis analysis by flow cytometry. The cell suspension was made from 1 to 2 mm^3 of tumor tissue from each individual group. Cells were washed three times by 0.1 mol/L PBS and fixed by 70% ethanol. Cells were then incubated with 50 mg/L PI, 1.0% Triton X-100 and 10 mg/L RNaseA for 30 min at 4°C in dark. Apoptosis and cell cycle distribution were analyzed by flow cytometry.[21] Proliferation index (PI) = $(S+G_2/M)/(G_0/G_1+S+G_2/M)$.

TUNEL assay for detection of in situ apoptosis. Liver tumor sections (4 μm) were fixed using 4% PFA, followed by digestion with 0.02 mg/L proteinase K for 30 min at room temperature. Sections were soaked in 3% H_2O_2 for 5 min at room temperature to deactivate endogenous peroxidases. Sections were then soaked in balance buffer for 20 min, followed by incubation with a solution containing 1:20 terminal deoxynucleotidyl transferase (TDT) enzyme at 37°C for 1.5 h. After washing, the antibody was added and incubated for 30 min at 37°C. Diaminobenzidine was used to develop the section after a second round of washing. Negative control was performed by using ddH_2O instead of TDT. Apoptotic cells were recognized if the nucleus stained brown or tan.[22,23] At least 1,000 cells were counted by DMR+Q550 system (Laica) from at least 10 scopes. The apoptotic index (AI) was calculated accordingly.

Statistics. All data was collected and expressed as an average ± standard deviation. ANOVA was used to analyze data within the same group, one-way ANOVA was used to analyze data between groups, while the LSD method was used for pairwise comparison between groups. A value of $\alpha = 0.05$, $p < 0.05$ was considered statistically significant.

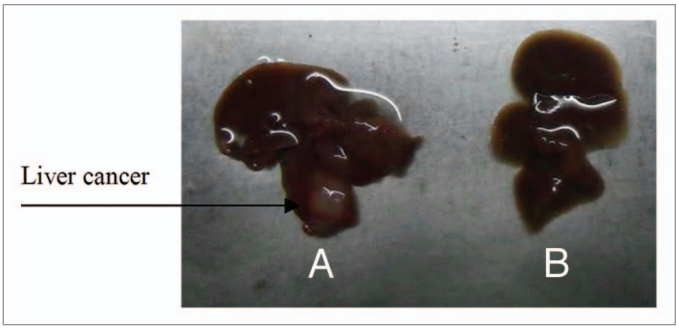

Figure 9. Establishment of the hepatic cancer mouse model. (**A**) Liver cancer; (**B**) normal mouse liver.

Conclusion

We demonstrated that GC is a good carrier for nano-material, especially 5-FU. GC/5-FU nanoparticles is a sustained release and highly targeted drug with lower toxicity, its peak time, half-life time, mean residence time and AUC were longer or more than those of 5-FU. GC/5-FU is an effective drug on liver cancer with high targeting and less toxicity. GC/5-FU nanoparticles can also significantly inhibit the tumor growth in the orthotropic liver cancer mouse model, and this in vivo effect was stronger than that of 5-FU alone. The mechanism underlying GC/5-FU nanoparticles was concluded to be elevated G_0-G_1 arrest and apoptosis.

Disclosure of Potential Conflicts of Interest

No potential conflicts of interest were disclosed.

Acknowledgments

This work was supported by Natural Science Foundation of Shanghai (09ZR1424700 and 114119a4700); Minhang District Natural Science Foundation of Shanghai (2009MHZ085); Minhang District Public Health Bureau Foundation of Shanghai (2009MW28).

References

1. Kim NH, Kim SN, Oh JS, Lee S, Kim YK. Anti-mitotic potential of 7-diethylamino-3(2'-benzoxazolyl)-coumarin in 5-fluorouracil-resistant human gastric cancer cell line SNU620/5-FU. Biochem Biophys Res Commun 2012; 418:616-21; PMID:22301191; http://dx.doi.org/10.1016/j.bbrc.2012.01.049.
2. Hsieh CH, Liu CY, Hsieh YJ, Tai HC, Wang LY, Tsai TH, et al. Matrix metalloproteinase-8 mediates the unfavorable systemic impact of local irradiation on pharmacokinetics of anti-cancer drug 5-Fluorouracil. PLoS One 2011; 6:e21000; PMID:21695264; http://dx.doi.org/10.1371/journal.pone.0021000.
3. Namikawa T, Fukudome I, Kitagawa H, Okabayashi T, Kobayashi M, Hanazaki K. Plasma diamine oxidase activity is a useful biomarker for evaluating gastrointestinal tract toxicities during chemotherapy with oral fluorouracil anti-cancer drugs in patients with gastric cancer. Oncology 2012; 82:147-52; PMID:22433290; http://dx.doi.org/10.1159/000336799.
4. Sakata Y, Komatsu Y, Takagi S, Saitoh S, Itoh T, Suzuki H, et al. Randomized controlled study of mitomycin C/carboquone/5-fluorouracil/OK-432 (MQ-F-OK) therapy and mitomycin C/5-fluorouracil/doxorubicin (FAM) therapy against advanced liver cancer. Cancer Chemother Pharmacol 1989; 23(Suppl):S9-12; PMID:2647315; http://dx.doi.org/10.1007/BF00647230.
5. Kanetaka K, Enjoji A, Furui J, Nagata Y, Fujioka H, Shiogama T, et al.; The Nagasaki Study Group for Digestive Organ Cancer Chemotherapy. Effects of Intermittent 5-Fluorouracil and Low-dose Cisplatin Therapy on Advanced and Recurrent Gastric Cancer. Anticancer Res 2012; 32:3495-9; PMID:22843936.
6. Sinha VR, Honey. Critical aspects in rationale design of fluorouracil-based adjuvant therapies for the management of colon cancer. Crit Rev Ther Drug Carrier Syst 2012; 29:89-148; PMID:22577701; http://dx.doi.org/10.1615/CritRevTherDrugCarrierSyst.v29.i2.10.
7. Kurosaki I, Kawachi Y, Nihei K, Tsuchiya Y, Aono T, Yokoyama N, et al. Liver perfusion chemotherapy with 5-Fluorouracil followed by systemic gemcitabine administration for resected pancreatic cancer: preliminary results of a prospective phase 2 study. Pancreas 2009; 38:161-7; PMID:18797423; http://dx.doi.org/10.1097/MPA.0b013e31818815f7.

8. Zhao HY, Huang H, Hu ZH, Huang Y, Lin SX, Tian Y, et al. Evaluations of biomarkers associated with sensitivity to 5-fluorouracil and taxanes for recurrent/advanced breast cancer patients treated with capecitabine-based first-line chemotherapy. Anticancer Drugs 2012; 23:534-42; PMID:22481060; http://dx.doi.org/10.1097/CAD.0b013e32834f7ef4.
9. White RM. Correct fluorouracil (5-FU) half-life comparator for a 5-FU prodrug plus a dihydropyrimidine dehydrogenase inhibitor. J Clin Oncol 2001; 19:2970; PMID:11387375.
10. Dikken C, Sitzia J. Patients' experiences of chemotherapy: side-effects associated with 5-fluorouracil + folinic acid in the treatment of colorectal cancer. J Clin Nurs 1998; 7:371-9; PMID:9830978; http://dx.doi.org/10.1046/j.1365-2702.1998.00159.x.
11. Wettergren Y, Carlsson G, Odin E, Gustavsson B. Pretherapeutic uracil and dihydrouracil levels of colorectal cancer patients are associated with sex and toxic side effects during adjuvant 5-fluorouracil-based chemotherapy. Cancer 2012; 118:2935-43; PMID:22020693; http://dx.doi.org/10.1002/cncr.26595.
12. Wilson B, Ambika TV, Dharmesh Kumar Patel R, Jenita JL, Priyadarshini SR. Nanoparticles based on albumin: Preparation, characterization and the use for 5-flurouracil delivery. Int J Biol Macromol 2012; PMID:22820011; http://dx.doi.org/10.1016/j.ijbiomac.2012.07.014.
13. Chandy T, Das GS, Rao GH. 5-Fluorouracil-loaded chitosan coated polylactic acid microspheres as biodegradable drug carriers for cerebral tumours. J Microencapsul 2000; 17:625-38; PMID:11038121; http://dx.doi.org/10.1080/026520400417676.
14. Zhu L, Ma J, Jia N, Zhao Y, Shen H. Chitosan-coated magnetic nanoparticles as carriers of 5-fluorouracil: preparation, characterization and cytotoxicity studies. Colloids Surf B Biointerfaces 2009; 68:1-6; PMID:19013060; http://dx.doi.org/10.1016/j.colsurfb.2008.07.020.
15. Lai LF, Guo HX. Preparation of new 5-fluorouracil-loaded zein nanoparticles for liver targeting. Int J Pharm 2011; 404:317-23; PMID:21094232; http://dx.doi.org/10.1016/j.ijpharm.2010.11.025.
16. Lai LF, Guo HX. Preparation of new 5-fluorouracil-loaded zein nanoparticles for liver targeting. Int J Pharm 2011; 404:317-23; PMID:21094232; http://dx.doi.org/10.1016/j.ijpharm.2010.11.025.
17. Kim TH, Park IK, Nah JW, Choi YJ, Cho CS. Galactosylated chitosan/DNA nanoparticles prepared using water-soluble chitosan as a gene carrier. Biomaterials 2004; 25:3783-92; PMID:15020154; http://dx.doi.org/10.1016/j.biomaterials.2003.10.063.
18. Fallon RJ, Danaher M, Saxena A. The asialoglycoprotein receptor is associated with a tyrosine kinase in HepG2 cells. J Biol Chem 1994; 269:26626-9; PMID:7929394.
19. Cheng M, Li Q, Wan T, Hong X, Chen H, He B, et al. Synthesis and efficient hepatocyte targeting of galactosylated chitosan as a gene carrier in vitro and in vivo. J Biomed Mater Res B Appl Biomater 2011; 99:70-80; PMID:21656667; http://dx.doi.org/10.1002/jbm.b.31873.
20. Chang CJ, Chen YH, Huang KW, Cheng HW, Chan SF, Tai KF, et al. Combined GM-CSF and IL-12 gene therapy synergistically suppresses the growth of orthotopic liver tumors. Hepatology 2007; 45:746-54; PMID:17326190; http://dx.doi.org/10.1002/hep.21560.
21. Wang XH, Liu BR, Qu B, Xing H, Gao SL, Yin JM, et al. Silencing STAT3 may inhibit cell growth through regulating signaling pathway, telomerase, cell cycle, apoptosis and angiogenesis in hepatocellular carcinoma: potential uses for gene therapy. Neoplasma 2011; 58:158-71; PMID:21275467; http://dx.doi.org/10.4149/neo_2011_02_158.
22. Dung TD, Chang HC, Chen CY, Peng WH, Tsai CH, Tsai FJ, et al. Zanthoxylum avicennae extracts induce cell apoptosis through protein phosphatase 2A activation in HA22T human hepatocellular carcinoma cells and block tumor growth in xenografted nude mice. Int J Mol Med 2011; 28:927-36; PMID:21874223.
23. Khurana A, McKean H, Kim H, Kim SH, McGuire J, Roberts LR, et al. Silencing of HSulf-2 expression in MCF10DCIS.com cells attenuate ductal carcinoma in situ progression to invasive ductal carcinoma in vivo. Breast Cancer Res 2012; 14:R43; PMID:22410125; http://dx.doi.org/10.1186/bcr3140.
24. Li DC, Zhong XK, Zeng ZP, Jiang JG, Li L, Zhao MM, et al. Application of targeted drug delivery system in Chinese medicine. J Control Release 2009; 138:103-12; PMID:19433120; http://dx.doi.org/10.1016/j.jconrel.2009.05.008.
25. Whitesides GM. The 'right' size in nanobiotechnology. Nat Biotechnol 2003; 21:1161-5; PMID:14520400; http://dx.doi.org/10.1038/nbt872.
26. Marcucci F, Lefoulon F. Active targeting with particulate drug carriers in tumor therapy: fundamentals and recent progress. Drug Discov Today 2004; 9:219-28; PMID:14980540; http://dx.doi.org/10.1016/S1359-6446(03)02988-X.
27. Alex SM, Rekha MR, Sharma CP. Spermine grafted galactosylated chitosan for improved nanoparticle mediated gene delivery. Int J Pharm 2011; 410:125-37; PMID:21396993; http://dx.doi.org/10.1016/j.ijpharm.2011.02.067.
28. Jiang H, Wu H, Xu YL, Wang JZ, Zeng Y. Preparation of galactosylated chitosan/tripolyphosphate nanoparticles and application as a gene carrier for targeting SMMC7721 cells. J Biosci Bioeng 2011; 111:719-24; PMID:21334972; http://dx.doi.org/10.1016/j.jbiosc.2011.01.012.
29. Kim JH, Kim YS, Park K, Lee S, Nam HY, Min KH, et al. Antitumor efficacy of cisplatin-loaded glycol chitosan nanoparticles in tumor-bearing mice. J Control Release 2008; 127:41-9; PMID:18234388; http://dx.doi.org/10.1016/j.jconrel.2007.12.014.
30. Yu BT, Sun X, Zhang ZR. Enhanced liver targeting by synthesis of N1-stearyl-5-Fu and incorporation into solid lipid nanoparticles. Arch Pharm Res 2003; 26:1096-101; PMID:14723346; http://dx.doi.org/10.1007/BF02994764.
31. Yan C, Gu J, Guo Y, Chen D. In vivo biodistribution for tumor targeting of 5-fluorouracil (5-FU) loaded N-succinyl-chitosan (Suc-Chi) nanoparticles. Yakugaku Zasshi 2010; 130:801-4; PMID:20519858; http://dx.doi.org/10.1248/yakushi.130.801.
32. Sasaki K, Tsuno NH, Sunami E, Tsurita G, Kawai K, Okaji Y, et al. Chloroquine potentiates the anti-cancer effect of 5-fluorouracil on colon cancer cells. BMC Cancer 2010; 10:370; PMID:20630104; http://dx.doi.org/10.1186/1471-2407-10-370.
33. Huang Z, Guo KJ, Guo RX, He SG. Effects of 5-fluouracil combined with sulfasalazine on human pancreatic carcinoma cell line BxPC-3 proliferation and apoptosis in vitro. Hepatobiliary Pancreat Dis Int 2007; 6:312-20; PMID:17548258.